Contract No:

This document was prepared in conjunction with work accomplished under Contract No. DE-AC09-08SR22470 with the U.S. Department of Energy.

Disclaimer:

FORMIC ACID FREE FLOWSHEET DEVELOPMENT TO ELIMINATE CATALYTIC HYDROGEN GENERATION IN THE DEFENSE WASTE PROCESSING FACILITY

Dan P. Lambert, Michael E Stone, and J. David Newell, Savannah River National Laboratory
Terri L. Fellinger and Jonathan M. Bricker, Savannah River Remediation, LLC
Aiken, SC, USA

Abstract

The Defense Waste Processing Facility (DWPF) processes legacy nuclear waste generated at the Savannah River Site (SRS) during production of plutonium and tritium demanded by the Cold War. The nuclear waste is first treated via a complex sequence of controlled chemical reactions and then vitrified into a borosilicate glass form and poured into stainless steel canisters. Converting the nuclear waste into borosilicate glass canisters is a safe, effective way to reduce the volume of the waste and stabilize the radionuclides.

Testing was initiated to determine whether the elimination of formic acid from the DWPF's chemical processing flowsheet would eliminate catalytic hydrogen generation. Historically, hydrogen is generated in chemical processing of alkaline High Level Waste sludge in DWPF. In current processing, sludge is combined with nitric and formic acid to neutralize the waste, reduce mercury and manganese, destroy nitrite, and modify (thin) the slurry rheology. The noble metal catalyzed formic acid decomposition produces hydrogen and carbon dioxide. Elimination of formic acid by replacement with glycolic acid has the potential to eliminate the production of catalytic hydrogen.

Flowsheet testing was performed to develop the nitric-glycolic acid flowsheet as an alternative to the nitric-formic flowsheet currently being processed at the DWPF. This new flowsheet has shown that mercury can be reduced and removed by steam stripping in DWPF with no catalytic hydrogen generation. All processing objectives were also met, including greatly reducing the Slurry Mix Evaporator (SME) product yield stress as compared to the baseline nitric/formic flowsheet. Ten DWPF tests were performed with nonradioactive simulants designed to cover a broad compositional range. No hydrogen was generated in testing without formic acid.

Introduction

Savannah River Remediation (SRR) is evaluating changes to its current DWPF flowsheet to improve processing cycle times. This will enable the facility to support higher canister production while maximizing waste loading. Higher throughput is needed in the CPC since the installation of the bubblers into the melter has increased melt rate. Due to the significant maintenance required for the DWPF gas chromatographs (GC) and the potential for production of flammable quantities of hydrogen, reducing or eliminating the amount of formic acid used in the CPC is being developed. Earlier work at Savannah River National Laboratory has shown that replacing formic acid with an 80:20 molar blend of glycolic and formic acids has the potential to remove mercury in

the SRAT without any significant catalytic hydrogen generation.[1,2,3] This report summarizes the research completed to determine the feasibility of processing without formic acid.

In earlier development of the glycolic-formic acid flowsheet, one run (GF8) 2 was completed without formic acid. It is of particular interest that mercury was successfully removed in GF8, no formic acid at 125% stoichiometry. Glycolic acid did not show the ability to reduce mercury to elemental mercury in initial screening studies, which is why previous testing focused on using the formic/glycolic blend.

The objective of the testing detailed in this document is to determine the viability of the nitric-glycolic acid flowsheet in processing sludge over a wide compositional range as requested by DWPF.[4] This work was performed under the guidance of Task Technical and Quality Assurance Plan (TT&QAP).[5] The details regarding the simulant preparation and analysis have been documented previously.[6]

Experimental Procedure

The experimental apparatus used in these experiments is typical for DWPF SRAT/SME testing. The four experiments were performed in 4-L kettles. The test equipment included a GC to measure off-gas composition, an ammonia scrubber, and a pH meter. In all runs, the SRNL acid calculation spreadsheet[7] used the Koopman equation[8] to determine acid addition quantities and dewater targets.

---

1 Pickenheim, B.R., M.E. Stone, SRAT Alternative Reductant Feasibility Assessment – Phase I, SRNL-STI-2009-00120, Savannah River National Laboratory, Aiken, SC, February 2009.

2 Pickenheim, B.R., M.E. Stone, J.D. Newell, Glycolic-Formic Acid Flowsheet Development, SRNL-STI-2010-00523, Rev 0, Savannah River National Laboratory, Aiken, SC, November 2010.

3 D.P. Lambert, B.R. Pickenheim, M.E. Stone, J.D. Newell, D.R. Best, Glycolic - Formic Acid Flowsheet Final Report for Downselection Decision, SRNL-STI- 2010-00523, Rev 1, Savannah River National Laboratory, Aiken, SC, March 2011.

4 Fellinger, T.L., "*Alternate Reductant Flowsheet Development – Phase I*", HLW-DWPF-TTR-2012-0003, Revision 0, October 2011.

5 Lambert, D.P., Task Technical and Quality Assurance Plan for Glycolic Acid Flowsheet Development, SRNL-RP-2011-01586, Savannah River National Laboratory, Aiken, SC, November 2011.

6 D. C. Koopman, D. P. Lambert, Initial Characterizations and SRAT Simulations of Four Sludge Matrix Study Simulants, SRNL-STI-2009-00606, Revision 0, Savannah River National Laboratory, Aiken, SC, December 2009

7 Lambert, D.P., Acid Calculation Spreadsheet for DWPF Simulations, Revision 1, SRNL-PSE-2006-00176, Savannah River Site, Aiken, SC 29808 (2006).

8 Koopman, D.C., A.I. Fernandez, B.R. Pickenheim, Preliminary Evaluations of Two Proposed Stoichiometric Acid Equations, Revision 0, Savannah River Site, Aiken, SC 29808 (2009).

CPC Simulation Details

The SRAT 4-L rigs were assembled following the guidelines of SRNL-3100-2011-00127.[1] The intent of the equipment is to functionally replicate the DWPF processing vessels. Each glass kettle is used to replicate both the SRAT and SME, and it is connected to the SRAT Condenser, the MWWT, and the FAVC. The Slurry Mix Evaporator Condensate Tank (SMECT) is represented by a sampling bottle that is used to remove condensate through the MWWT. For the purposes of this paper, the condensers and wash tank are referred to as the off-gas components. A sketch of the experimental setup is given in Figure 2-1.

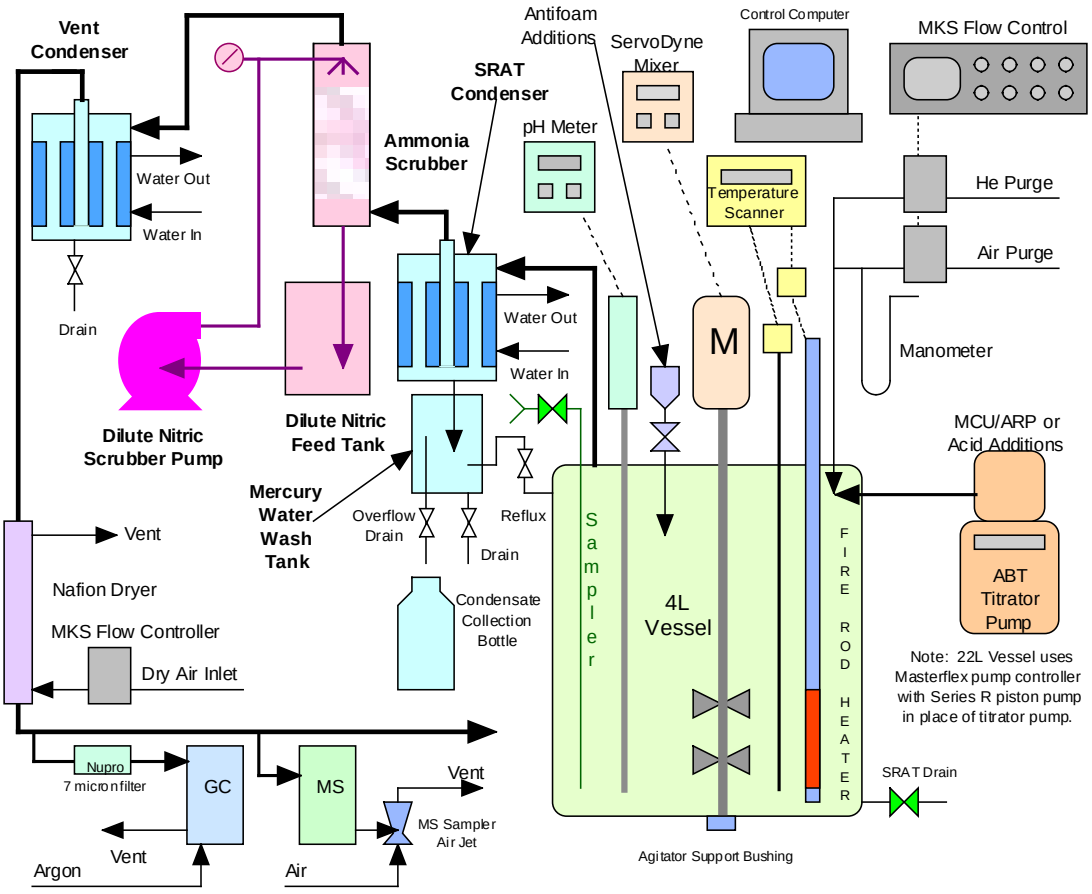

Figure 2-1. Schematic of CPC Equipment Set-Up

Concentrated nitric acid (~50 wt %) and glycolic acid (~70 wt %) were used to acidify the sludge and perform neutralization and reduction reactions during processing. The total amount of acid (in moles) to add for each run was determined using the Koopman acid equation[8]. The Koopman minimum acid equation was used with a 100% stoichiometric factor for all tests except GF38 (125%), GF40 (134%) and GF41 (130%).

---

[1] Stone, M. E., Lab-Scale CPC Equipment Set-up, SRNL-ITS-2006-000742011-00127, Savannah River Site, Aiken, SC 29808 (2011).

The acid mix was partitioned between nitric and glycolic acid by utilizing the latest REDOX equation[1] with a term added for glycolate ion (see below). A coefficient of 6 was used on the glycolate term based on electron equivalence.[2] The REDOX target ($Fe^{2+}/\Sigma Fe$) was 0.1. Process assumptions were made to predict SME product anion concentrations. In addition to the standard assumptions needed for formate and oxalate loss and nitrite to nitrate conversion, a factor was added to the acid calculation for glycolate loss. Process assumptions for the stoichiometric window testing were adjusted based on results from earlier testing.

$$REDOX=0.2358+0.1999*((2*C_{formate}+4*C_{oxalate}+4*C_{Carbon}+6*C_{glycolate}-5*(C_{Nitrate}+C_{Nitrite})-5*C_{Mn}))*(45/TS)$$

Where C_x = species concentration of component x, g-mole/kg melter feed, TS = total solids in melter feed in wt %, and REDOX is a molar ratio of $Fe^{2+}/\Sigma Fe$

A standard 4-L SRAT/SME apparatus with an ammonia scrubber was used for these simulations. The scrubber solution consisted of 749 g of de-ionized water and 1 g of 50 wt% nitric acid. The solution was recirculated through the column by a MasterFlex pump at 300 mL/min through a spray nozzle at the top of the packed section. Glass rings were used as packing and did not significantly add to the back pressure on the SRAT vessel as has been seen in earlier tests with different packing. The SRAT condenser was maintained at 25 °C during the run, while the vent condenser was maintained at 4 °C.

Sludge Preparation

SRNL produced four matrix sludge simulants in order to improve the understanding of how changing sludge composition impacts DWPF waste processing. These simulants have been used in other SRNL studies, and the composition has been previously measured.[3] These simulants were used to demonstrate the flowsheet across a broad compositional range. In addition, two less washed simulants (1.6 and 1.9 M Na) were produced to study the impact of less washing on CPC processing.

---

1 Jantzen, C. M. and M. E. Stone, Role of Manganese Reduction/Oxidation (REDOX) on Foaming and Melt Rate in High Level Waste Melters, WSRC-STI-2006-00066, Savannah River Site, Aiken, SC, 29808 , March 2007.

2 Jantzen, C.M., J.R. Zamecnik, D.C. Koopman, C.C. Herman, and J.B. Pickett, Electron Equivalents Model for Controlling Reduction-Oxidation (REDOX) Equilibrium during High Level Waste (HLW) Vitrification, WSRC-TR-2003-00126, Savannah River Site, Aiken, SC 29808 (2003).

3 Lambert, D. P., Koopman, D. C., Glycolic-Formic Acid Flowsheet Sludge Matrix Study, SRNL-STI-2011-00275, Savannah River Site, Aiken, SC, 29808 (June 2011).

Table 2-1. Composition of Sludge Simulants

Result	GF34 HiFeHiMn	GF35 SB7An	GF36 HiFeLoMn	GF37/38 LoFeLoMn	GF40 1.6 M Na	GF41 1.9 M Na	Units
Total Solids	23.70	18.02	22.81	23.07	24.14	25.43	wt%
Calcined Solids	17.81	13.61	16.95	16.00	17.01	17.85	wt%
Insoluble Solids	16.70	12.57	16.35	16.05	16.51	16.97	wt%
Soluble Solids	7.00	5.45	6.47	7.01	7.63	8.46	wt%
Slurry Density	1.185	1.142	1.189	1.176	1.174	1.215	kg / L slurry
Filtrate Density	1.057	1.053	1.055	1.057	1.076	1.091	kg / L supernate
Aluminum	9.000	15.65	9.130	23.8	14.8	13.9	wt % calcined basis
Boron	<0.100	<0.100	<0.100	<0.100	NM	NM	wt % calcined basis
Barium	0.077	0.102	0.101	0.0705	0.085	0.0802	wt % calcined basis
Calcium	3.83	0.836	2.22	1.97	0.565	0.288	wt % calcined basis
Cadmium	<0.010	NM	<0.010	<0.010	NM	NM	wt % calcined basis
Cerium	0.104	0.148	0.108	0.0965	NM	NM	wt % calcined basis
Chromium	0.015	0.0455	0.285	0.244	0.027	0.0260	wt % calcined basis
Copper	0.045	0.033	0.045	0.048	0.040	0.0350	wt % calcined basis
Iron	32.4	19.2	31.5	12.2	14.8	13.7	wt % calcined basis
Potassium	0.120	0.125	0.0905	0.0955	0.369	0.392	wt % calcined basis
Magnesium	0.396	0.366	2.69	2.42	0.317	0.302	wt % calcined basis
Manganese	4.04	4.37	0.721	0.661	4.86	4.53	wt % calcined basis
Sodium	12.9	15.3	13.1	14.2	22.8	24.4	wt % calcined basis
Nickel	0.213	3.37	2.6345	2.31	2.10	1.95	wt % calcined basis
Phosphorus	<0.100	<0.100	<0.100	<0.100	0.032	<0.010	wt % calcined basis
Lead	0.071	0.025	0.047	0.0715	<0.010	<0.010	wt % calcined basis
Sulfur	0.289	0.371	0.340	0.374	0.276	0.333	wt % calcined basis
Silicon	1.580	1.91	1.52	1.32	1.52	1.369	wt % calcined basis
Tin	<0.010	0.013	0.106	0.0925	NM	NM	wt % calcined basis
Titanium	<0.010	0.025	<0.010	<0.010	0.025	0.0230	wt % calcined basis
Zinc	0.065	0.047	0.0775	0.0705	0.049	0.0452	wt % calcined basis
Zirconium	0.054	0.252	0.1175	0.049	0.027	0.195	wt % calcined basis
Nitrite	17,900	9,140	17,800	13,300	13,500	15,800	mg/kg slurry
Nitrate	13,550	6,470	13,400	13,300	7,895	9,940	mg/kg slurry
Formate	<100	<100	<100	<100	<100	<100	mg/kg slurry
Sulfate	1,770	1,460	1,575	1,590	1,980	2,610	mg/kg slurry
Chlorine	116	<100	131	127	<100	<100	mg/kg slurry
Phosphate	0	<100	<100	<100	<100	<100	mg/kg slurry
Oxalate	300	8,500	275	295	18,750	20,000	mg/kg slurry
Glycolate	<100	NM	<100	<100	<100	<100	mg/kg slurry
Slurry TIC	2,751	1,066	2,492	2,400	1,840	1,730	mg/kg slurry
Supernate TIC	1,080	664	1,310	1,280	1,790	1760	mg/L supernate
Total Base pH 7	0.590	0.580	0.562	0.522	0.838	0.879	moles/L

Table 2-2. Mercury and Noble Metal Composition Added to Sludge Simulants, wt% Total Solids Basis

Noble Metal	Runs GF34-GF38	GF40-41
Target Hg	1.5000	1.500
Target Ag	0.0014	0.0144
Target Pd	0.0790	0.0033
Target Rh	0.0380	0.0192
Target Ru	0.2170	0.0877

An additional supernate simulant was prepared to supplement the four slurry simulants above. The purpose of this simpler simulant was to improve understanding of the mercury reduction chemistry. The simulant was similar to the supernate used in the matrix slurry preparation. The only soluble species added were sodium hydroxide, sodium nitrite, sodium nitrate, sodium sulfate, sodium oxalate, sodium carbonate and potassium nitrate. The resulting concentration is summarized in Table 2-3. The added noble metal and mercury target of these runs is summarized in Table 2-4. Note that because of the lower total solids of the supernate, the added mass of noble metals and mercury is approximately one-third that added in the slurry experiments.

Table 2-3. Composition of Supernate Simulant

Anion or Cation	GF39a-d	GF39e
Nitrite, mg/kg	21,561	0
Nitrate, mg/kg	15,784	16,311
Carbonate, mg/kg	6,051	6,253
Oxalate, mg/kg	351	363
Sulfate, mg/kg	1,888	1,951
Free Hydroxide, M	3,556 (0.221 M)	0.221
Na, mg/kg	27,067	27,067
K, mg/kg	153	153

Table 2-4. Mercury and Noble Metal Composition Added to Supernate Simulants, wt% Total Solids Basis

Noble Metal	GF39a	GF39b	GF39c	GF39d	GF39e
Target Hg	1.5000	1.5000	1.5000	1.5000	2.5717
Target Ag	0.0000	0.0014	0.0014	0.0014	0.0000
Target Pd	0.0000	0.0790	0.0790	0.0790	0.0000
Target Rh	0.0000	0.0297	0.0297	0.0297	0.0000
Target Ru	0.0000	0.2170	0.0000	0.2170	0.0000

CPC Run Details

The twelve nitric-glycolic acid flowsheet tests with slurry and five tests with supernate were performed at the ACTL using the four-liter kettle setup. Table 2-5 identifies each run and its corresponding assumptions.

Table 2-5. CPC Simulation Process Assumptions

Run	Sludge	Cycles	Date	% Koopman Acid Stoichiometry
GF34	HiFeHiMn	SRAT/SME	16-Nov-11	104.0
GF34b	HiFeHiMn	SRAT/SME	16-Nov-11	104.0
GF34c	HiFeHiMn	SRAT/SME	16-Nov-11	104.0
GF35	SB7A	SRAT/SME	17-Nov-11	100.0
GF36	HiFeLoMn	SRAT/SME	16-Nov-11	106.1
GF36b	HiFeLoMn	SRAT	25-Jan-12	106.1
GF36c	HiFeLoMn	SRAT	25-Jan-12	106.1
GF37	LoFeLoMn	SRAT/SME	2-Feb-12	100.0
GF37b	LoFeLoMn	SRAT	17-Nov-11	100.0
GF38	LoFeLoMn	SRAT	2-Feb-12	125.0
GF39A	Supernate	SRAT	22-Feb-12	100.0
GF39B	Supernate	SRAT	22-Feb-12	100.0
GF39C	Supernate	SRAT	29-Feb-12	100.0
GF39D	Supernate	SRAT	29-Feb-12	80.0
GF39E	No Nitrite Supernate	SRAT	8-May-12	100.0
GF40	1.6M Na	SRAT	24-May-12	133.9
GF41	1.9 M Na	SRAT	24-May-12	130.0

DWPF design basis processing conditions were scaled down and used for most processing parameters including SRAT/SME air purges and boil-up rate. SRAT product total dried solids were targeted at 27 wt% for the slurry simulant runs. Final SME total dried solids were targeted at 45% at 36% waste loading.

Because nitric and glycolic acid are more dilute acids than formic acid, both acids were added at the same molar flowrate as formic acid. Thus nitric acid was added at a DWPF scaled flowrate of 4.572 gallons per minute and glycolic acid was added at a DWPF scaled flowrate of 3.948 gallons per minute to maintain acid addition times. It is recommended that DWPF modify the acid feed pumps to deliver the higher flow rates before implementing the glycolic flowsheet.

The following constraints must be met by the current DWPF CPC flowsheet:

- SRAT hydrogen <0.65 lb/hr
- SME hydrogen <0.223 lb/hr
- Reduce mercury to elemental form
- Steam strip mercury below 0.8 wt% in the SRAT product dried solids
- SRAT product less than 1000 mg nitrite/kg product slurry

- SRAT product rheology[13] design basis 1.5 to 5 Pa yield stress and 5 to 12 cP consistency
- SME product rheology[1] 2.5 to 15 Pa yield stress and 10 to 40 cP consistency
- Glass REDOX of 0.09-0.33 $Fe^{2+}/\sum Fe$
- Minimize water in SME product (55 wt% typical)
- Minimal foaming

Twelve to fifteen samples were taken during each SRAT cycle to monitor the progress of the main chemical reactions. Major cations and anions were checked immediately after acid addition. Samples were taken during boiling to monitor suspended and dissolved mercury in the SRAT slurry. These samples were transferred directly into digestion vials to eliminate potential segregation of mercury during sub-sampling/aliquoting steps. The SRAT and SME product slurries were sampled similarly once they had cooled to 90° C while the vessel contents were still mixing.

Additional SRAT product samples were taken for compositional and solids analyses after the product had cooled further. The MWWT and FAVC were drained and the condensates weighed after both the SRAT and SME cycles. Elemental mercury was separated from the aqueous phase in the post-SRAT MWWT sample, and the mass of the mercury-rich material determined. Beads of elemental mercury were also recovered from a few of the SME dewatering condensates and weighed (depending on how big or numerous the bead(s) appeared to be).

Data are presented in Section 3 showing how the nitric-glycolic flowsheet met or exceeded the processing constraints in the list above with the possible exception of mercury removal and REDOX.

Results and Discussion

Four SRAT simulations with supernate and eight SRAT/SME process simulations with slurry feeds were completed to demonstrate the feasibility of using only glycolic acid as the reducing acid in SRAT processing. The elimination of formic acid has the potential to eliminate the catalytic generation of hydrogen, which could lead to the reduction of the air purge in the DWPF CPC. The main concern in eliminating formic acid[1] is that the mercury won't be effectively reduced, and won't be removed by steam stripping to meet the DWPF SRAT mercury target and minimize the mercury sent to the melter. The discussion begins with the supernate results followed by the slurry results.

Supernate Testing

Four SRAT process simulations were completed with a simple supernate solution with added mercury and noble metals. A fifth run was completed with a nitrite free supernate solution to determine whether nitrite is needed to reduce mercury. These runs were performed after the slurry runs in order to better understand the processing chemistry. In particular, it was important to understand when the mercury is reduced in processing. Samples were pulled during glycolic acid addition and for several hours during the dewater and reflux phases to better understand the process chemistry using a simpler mixture than sludge simulants.

[1] Processing limits are the same for both SRAT and SME as agitator and drive are identical.

Mercury Reduction and Stripping

Approximately 3.4 g of mercury were added to each simulation. The mercury recovery results are summarized in **Table 3-6**.

Table 3-6. Supernate Testing with Mercury and Noble Metals

Run	GF39a	GF39b	GF39c	GF39d	GF39e
Hg, wt %	1.5	1.5	1.5	1.5	1.5
Rh, wt %	0	0.0297	0.0297	0.0297	0
Pd, wt %	0	0.079	0.079	0.079	0
Ag, wt%	0	0.0014	0.0014	0.0014	0
Ru, wt %	0	0.3358	0	0.3358	0
% Koopman Acid Stoichiometry	100	100	100	80	100
% Hsu Acid Stoichiometry	74	74	74	60	58
Hg Collected, g	0.62*	None	0.43#	None	0.98

* Found 1.455 g of elemental Hg in kettle

Found 1.939 g of black solids in kettle

The runs demonstrated that the mercury could be reduced and stripped with only glycolic acid (no formic acid). The exception to this is that in the runs with added ruthenium chloride (GF39b, GF39d), no mercury was recovered. Based on the obvious color changes (see photos below), the mercury was likely reduced in all the supernate runs. In runs with added ruthenium, 0.765 g Ru was added as $RuCl_3 \cdot 1.93H_2O$ (1.832 g or 0.0227 g-moles of Cl). In all runs, 3.689 g of HgO were added (0.0170 g-moles of Hg). In previous testing, the presence of Cl led to the production of calomel (Hg_2Cl_2), which is not steam stripped. It is recommended that these runs should be repeated with another form of Ru such as ruthenium oxide hydrate to see if adding the Ru without Cl has the same impact on mercury stripping.

The mercury (II) contained in the starting slurry as mercuric oxide was reduced during the glycolic acid addition at a pH of approximately 4.5. The photographs below (Figure 3-1) show the slurry both before and after the run from Run GF39a (mercury was added but no noble metals). The kettle contents quickly changed from the orange HgO slurry to a transparent silver colored solution over a period of several minutes. The silver color slowly disappeared during boiling when the mercury was being steam stripped and recovered in the MWWT.

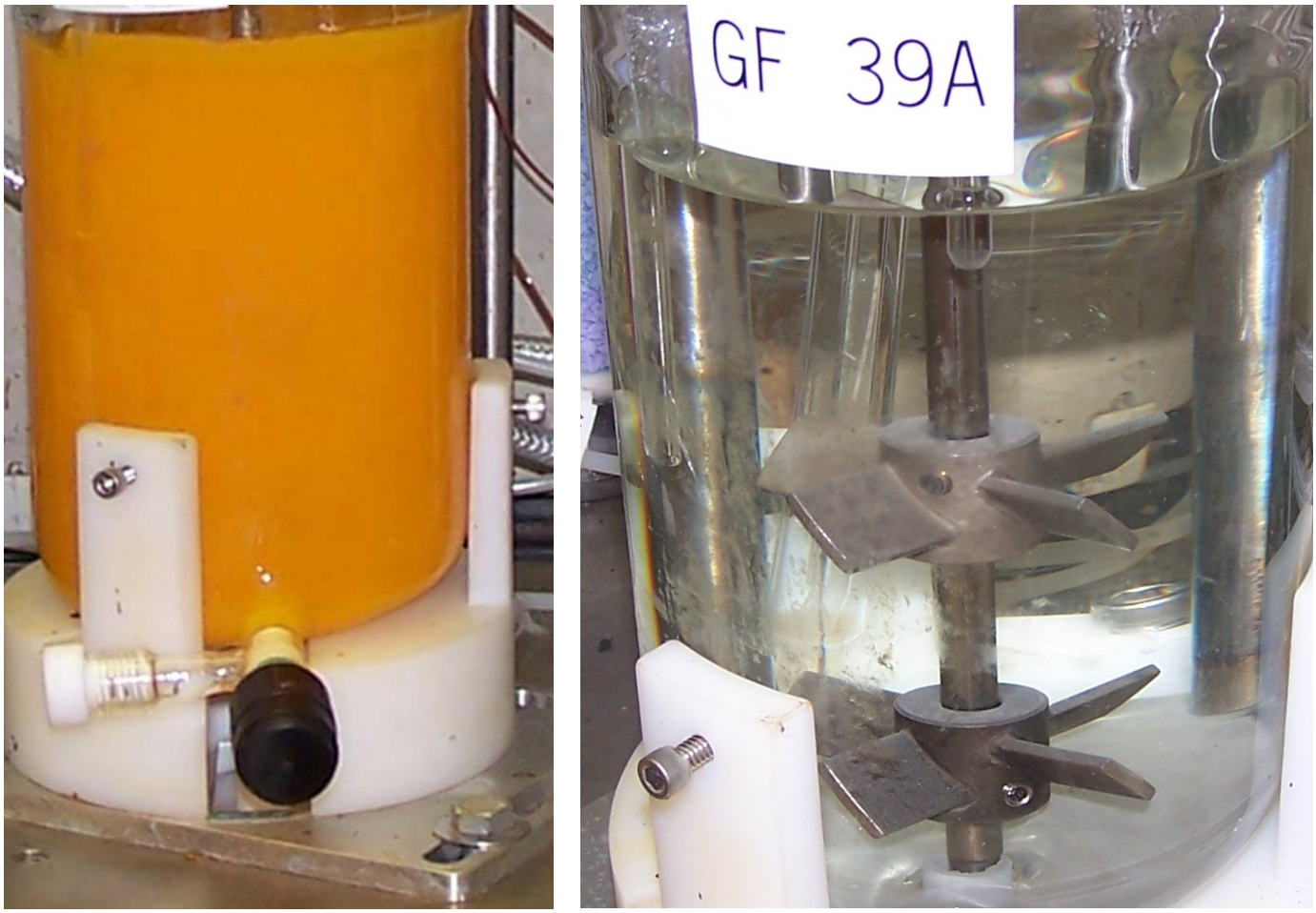

Figure 3-2. Photographs of GF39a before and after SRAT cycle (Supernate plus HgO)

In the runs with added noble metals and mercury, the slurry looked very much like sludge. The photographs below (Figure 3-2) show the slurry both before and after the run from Run GF39b (mercury and noble metals were added). The kettle contents quickly changed from the brown slurry to a transparent brown colored solution over a period of several minutes at a pH of 4.3. No mercury was recovered in the MWWT.

Figure 3-3. Photographs of GF39b before and after SRAT cycle (Supernate plus HgO and noble metals)

A mass balance was performed for each run to predict the concentration of all cations and anions throughout the run. In run GF39b (100% Koopman Stoichiometry, added noble metals and mercury), there was an apparent mass loss of 986 g (expected mass loss 151 g). This was calculated to match the final sodium concentration measured in the SRAT product sample. Using this mass loss, the predicted mercury concentration in the SRAT product is 2,306 mg/L and the measured mercury concentration was 2,315 mg/L. In other words, the mercury was completely soluble in the SRAT product and no mercury was recovered (not reduced, not stripped) in the MWWT. In contrast, run GF39a (100% Koopman stoichiometry, add mercury only), the final mercury concentration in the SRAT product was 14.9 mg/L compared to a predicted concentration of 1,433 mg/L (1.04% of the mercury was soluble). In addition, of the 3.4 g of mercury added initially on an elemental basis, 0.6 g was collected in the MWWT and 1.5 g was found in the SRAT product slurry as elemental mercury.

Nitrite and Carbonate Destruction

Nitrite and carbonate were below detection limits by the first hour of reflux in supernate testing. The results are summarized in Table 3-2.

Table 3-7. Nitrite Data, mg/L

Anion	GF39a	GF39b	GF39c	GF39d	GF39e
Post Nitric Acid	20,000	19,700	21,800	21,700	<500
Mid Glycolic Acid	10,800	6,560	4,540	11,700	<500
Post Glycolic Acid	<100	1,070	1,150	2,615	<500
1 hour dewater	<100	<100	<100	224	<500
Post Dewater	<100	<100	<100	<100	<500
Post Run	<100	<100	<100	<100	<500

Anion and Cation Mass Balance

Anions and cations were measured (solid lines in graphs below) throughout the supernate runs. A mass balance was completed for each run based on the known amounts added in preparing the supernate and the mass of added noble metals and mercury. These predictions (dotted lines), calculated by mass balance, were plotted along with the measured result in Figure 3-3 and Figure 3-4 (GF39b is presented as an example of this data). It should be noted that the PSAL measured nitrate agrees well with the nitrate prediction and the PSAL measured glycolate is approximately 20% higher than the prediction. In addition, oxalate is also much higher than predicted. It is likely that some oxalate is produced from glycolate decomposition. The measured nitrate is greater than predicted during glycolic acid addition due to the oxidation of nitrite to nitrate but is lower than predicted during reflux and boiling due to nitrate destruction. The sulfate concentration as measured by IC was very different than predicted. However, the measured sulfate, as calculated from ICP-AES S, was approximately 30% higher than predicted.

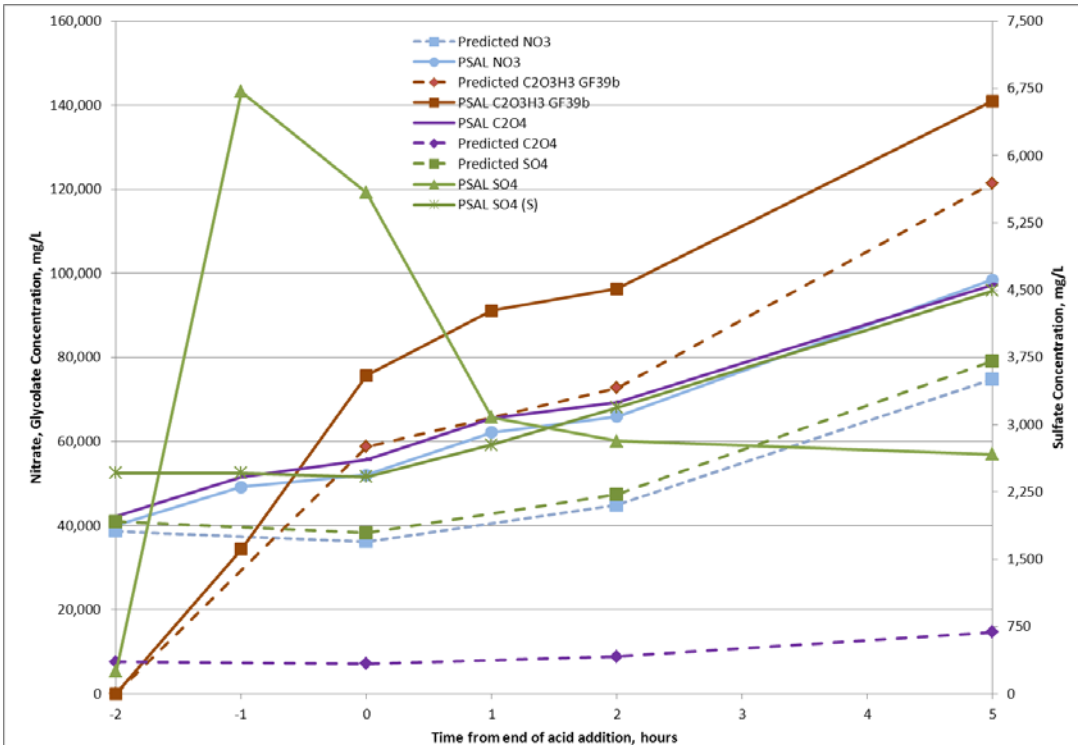

Figure 3-4. Supernate Run GF39b Predicted and Measured Anion Concentration

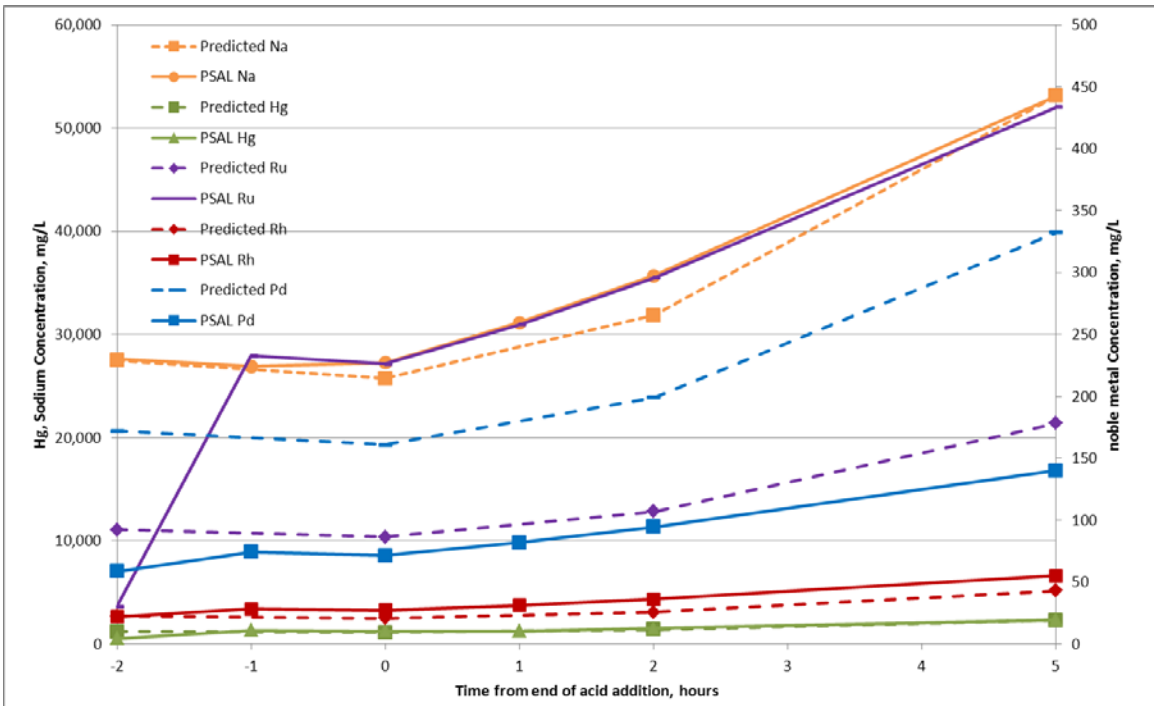

Figure 3-5. Supernate Run GF39b Predicted and Measured Cation Concentration

The measured sodium and mercury concentrations agreed well with predictions throughout run GF39b. The concentration of Pd and Ru were higher than predicted in Run GF39b. The Rh was approximately 80% of the predicted value and the Ag was below the detection limit. In Run GF39a (no added noble metals), the noble metals were all below detection limits.

Nitrite-free Supernate Test

One question that has always bothered our research team is whether glycolic acid is able to reduce mercury, allowing the elemental mercury to be removed by steam stripping. One theory was that glycolic acid needed a more reducing form such as glyoxylic acid to reduce the mercury. Glyoxylic acid, a better reducing agent than glycolic acid, could be produced by the reduction of glycolic acid by nitrite. As a result, a run was completed with a nitrite free simulant. This run was noble metal free, only mercury was added to the supernate. The result was that the mercury was completely reduced, a virtual duplication of Run GF39a. It appears that glycolic acid is fully capable of reducing mercury with or without nitrite present.

Slurry Testing

Twelve SRAT and six SME process simulations were completed to demonstrate the Glycolic-Nitric Flowsheet. Ten SRAT and four SME process simulations utilized the matrix sludges with added mercury and noble metals. Runs GF34, GF35, GF36 and GF37 were completed first and also included SME cycles. Runs 36b and 36c were duplicates of the GF36 SRAT cycle to compare the old and new processing rigs and determine whether the changes had impacted process chemistry. Run 37b was a duplicate of GF37 and GF38 was a higher acid stoichiometry repeat of GF37. The main reason for the four repeat runs was to better track mercury as the mercury

recovery in the first four runs was poor. Runs 34b and 34c were duplicates of the GF34 SRAT cycle to determine whether lowering the purge impacted process chemistry. In addition, runs GF40 and GF41 were SRAT and SME process simulations designed to determine whether the Glycolic-Nitric Acid flowsheet could successfully process the less washed simulants. Some data from the supernate runs is included in this section for completeness if they were not reported in Section 3.1.

Off-Gas Hydrogen

A main objective of this testing was to show that hydrogen generation could be mitigated or eliminated by the use of the glycolic/nitric flowsheet. Hydrogen was detected only in the GF40 and 41 SRAT cycles. These two runs had the "new lower purge" which led to higher measured hydrogen concentrations for a given generation rate. The GC hydrogen quantitation limit is 0.005 volume %. The maximum hydrogen detected in these runs was 0.009 volume %, which would have been below detection limits with the current DWPF scaled purge. Note that these runs were completed at approximately 130% stoichiometry and produced approximately 1% of the hydrogen compared to essentially identical runs with the Baseline flowsheet. Table 3-3 compares SRAT and SME cycle hydrogen on a DWPF scale. (Figure 3-5) summarizes the SRAT cycle hydrogen generation.

In the first four SME cycles (GF34, GF35, GF36, and GF37), formic acid was added with the frit in the SME cycle. In these runs, measurable hydrogen was generated, on the order of 0.05 volume percent. No formic acid was added in the GF40 and GF41 SME cycles. The GF41 hydrogen generation was just above quantitation limits in the GF40 SME cycle. In essentially identical runs with the Baseline flowsheet, the SME hydrogen limit was exceeded in runs at 125 and 130% acid stoichiometry.

Table 3-8. Peak Hydrogen Generation

Run	Sludge Composition	SRAT H2, lb/hr	SME H2, lb/hr
DWPF	Current Limit	0.65	0.223
GF34	HiFeHiMn	<0.0014	0.00556
GF34b	HiFeHiMn	<0.0014	No SME
GF34c	HiFeHiMn	<0.0014	No SME
GF35	SB7A	<0.0014	0.00398
GF36	HiFeLoMn	<0.0014	0.0111
GF37b	HiFeLoMn	<0.0014	No SME
GF37c	HiFeLoMn	<0.0014	No SME
GF37	LoFeLoMn	<0.0014	0.0157
GF37b	LoFeLoMn	<0.0014	No SME
GF38	LoFeLoMn	<0.0014	No SME
GF39a, b, c, d, e	Supernate	<0.0014	No SME
GF40	1.6 M Na	0.00287	0.00184
GF41	1.9 M Na	0.00324	<0.0012

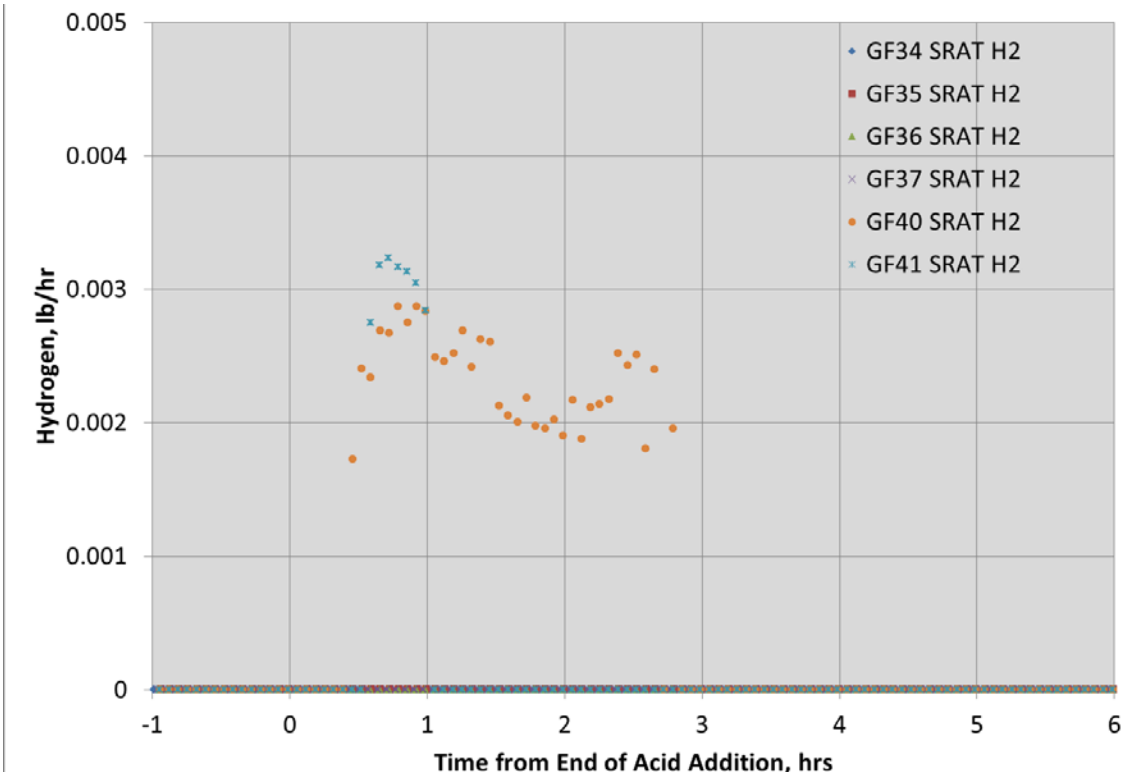

Figure 3-6. SRAT Cycle Hydrogen Generation

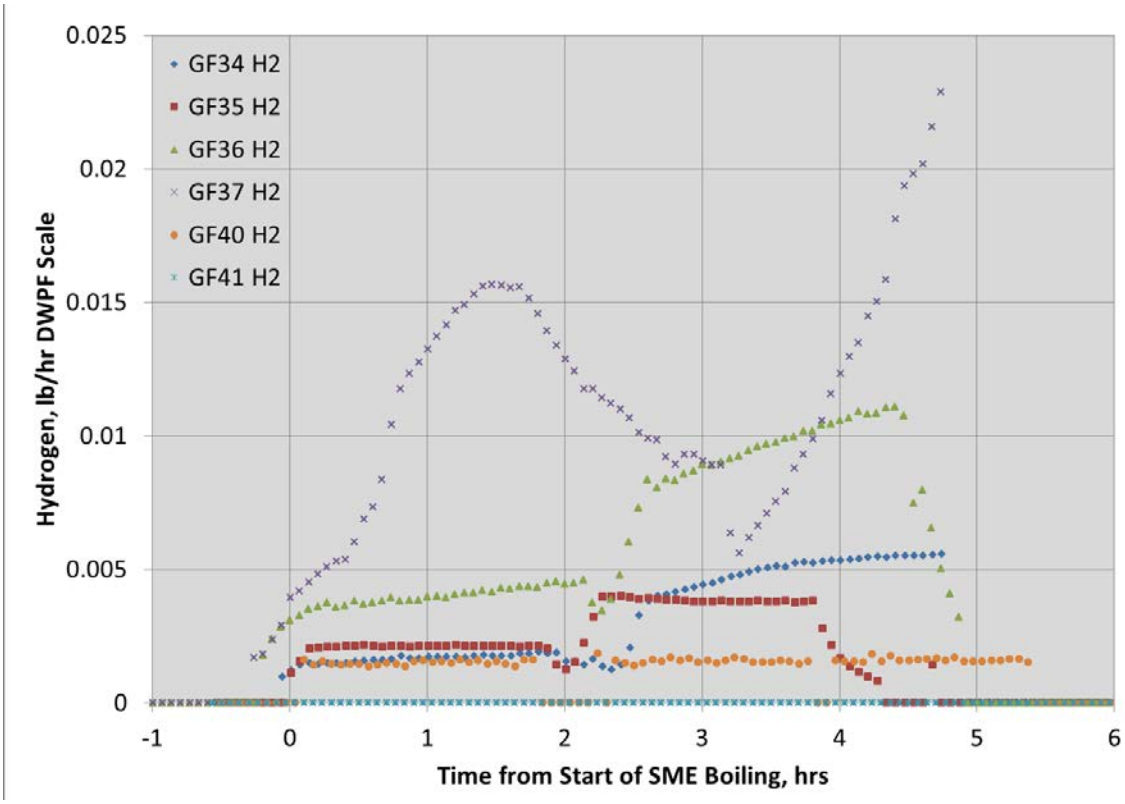

Figure 3-7. SME Cycle Hydrogen Generation

SRAT Mercury Reduction and Stripping

One of the most important questions to resolve concerning the glycolic-nitric acid flowsheet is whether mercury could be effectively reduced and steam stripped in the SRAT cycle without formic acid. In the Baseline flowsheet, mercury is reduced to elemental mercury during formic acid addition and then removed from the slurry by steam stripping during the concentration and reflux periods in SRAT processing.

The starting sludge was trimmed to 1.5 wt% Hg in the total solids. This required a theoretical boiling time of 12 hours to remove mercury to less than 0.80 wt% in the SRAT product total solids using lab-scaled DWPF design basis boil-up rates and a stripping efficiency of 750 g steam/g Hg.

A mass balance was completed for each of the runs to attempt to determine where the mercury had accumulated. The mercury mass balance is summarized in Table 3-7. In three of the first four runs, GF34, 35, 36 and 37, the mercury recovery was poor in the MWWT. As a result, Runs 34, 36 and 37 were repeated (Runs GF34b, GF34c, GF36b, GF36c, GF37b and GF38). The mercury recovery in the second set of runs was typical for lab-scale SRAT cycles[1]. No cause for the differences in duplicate runs has been identified, but it is possible that there was technician error in collecting the mercury. Run GF35 (SB7A sludge) was not repeated, since the sludge was consumed in Run GF35. Run GF38 was performed at 125% acid stoichiometry to determine if acid stoichiometry impacted mercury recovery. Note that about 50% less mercury was recovered in the MWWT in run GF38 (125% acid stoichiometry) than was recovered in run GF37b (100% acid stoichiometry). This phenomenon is also seen in Baseline flowsheet runs.

Two SRAT and SME cycles (GF40 and GF41) were performed with two underwashed SB8 simulants to demonstrate that mercury can be reduced without formic acid in glycolic flowsheet runs with typical (not matrix) sludge simulant. These runs were completed in parallel with two Baseline flowsheet runs. The Glycolic-Nitric Flowsheet runs both had higher mercury recovery in the MWWT (same Koopman acid stoichiometry, same noble metals and mercury, essentially duplicate runs). In all Glycolic-Nitric acid flowsheet testing, the mercury stripping and recovery in the MWWT has either met or exceeded the recovery in the Baseline flowsheet runs.

---

[1] Zamecnik, J.R., Behavior of Mercury during DWPF Chemical Process Cell, SRNL-STI-2012-00051, REVISION 0, Savannah River National Laboratory, Aiken, SC, April 2012.

Table 3-9. Mercury Balance in SRAT and SME Cycle, g

Run	% Acid Koopman	Added	MWWT	Slurry	Condensate	Total	% Recovery
GF34	104.0	10.56	2.27	12.12	2.27	16.66	160%
GF34b	104.0	10.56	5.89	6.36	NM	12.3	116%
GF34c	104.0	10.56	1.94	7.10	NM	9.04	86%
GF35	100.0	8.25	0.02	0.19	0.17	0.38	4.6%
GF36	106.1	10.17	0.14	5.85	0.53	6.52	64%
GF36b	106.1	10.17	2.27	6.59	NM	8.85	87%
GF36c	106.1	10.17	2.35	7.17	NM	9.53	94%
GF37	100.0	10.28	0.01	7.13	0.48	7.62	74.%
GF37b	100.0	10.28	4.10	4.75	NM	8.56	86%
GF38	125	10.28	1.99	7.40	NM	9.15	91%
GF40	130	11.15	3.79	5.21	0.44	9.44	85%
GF41	130	11.15	3.24	5.34	0.46	9.03	81%

Samples were taken periodically throughout the runs for mercury analysis. The chart below (Figure 3-15) shows the concentration of mercury in the slurry as a function of time for the eight runs. It is expected that the mercury concentration will decrease linearly during SRAT steam stripping and collect in the MWWT. A linear decrease of Hg concentration in the slurry assumes a constant boil-up rate and a constant approach to thermodynamic vapor-liquid equilibrium between the slurry and off-gas phases. The general trend of the mercury profile curves is a linear decrease as expected. It was expected that the SRAT product would have a mercury concentration of 0.8 wt% or 2160 mg/kg. The SRAT product Hg concentration ranged from 0.01-0.92 wt % total solids basis. Results are summarized Table 3-9.

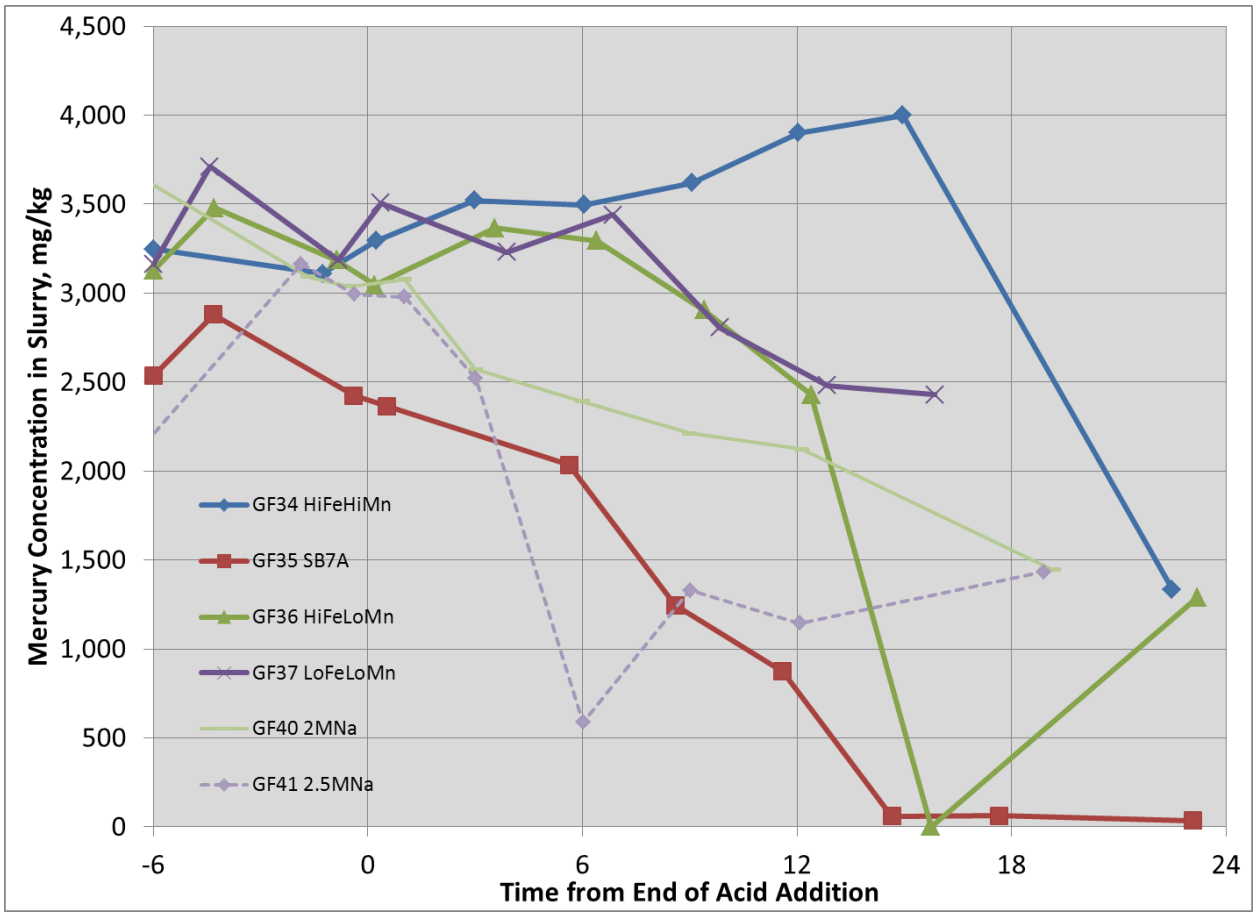

Figure 3-8. Mercury concentration versus time in Selected SRAT and SME cycles

Mercury is added to the sludge as HgO. In these runs the HgO was slurried with water and homogenized using the vortex mixer to break up any clumps and allow an even dispersal of the mercury. During SRAT processing the mercury is first dissolved and may later be reduced to elemental mercury. Once it is reduced, it is insoluble and can be steam stripped. In Runs GF37b and GF38, extra samples were pulled during the acid addition and dewater phase to understand when these reactions occur. In both runs, approximately 90% of the mercury was dissolved prior to the completion of nitric addition and the Hg was completely dissolved by midway through the glycolic acid addition. The mercury then is reduced during the first two hours of dewatering (faster during GF38, the 125% acid stoichiometry run, than during GF37b, the 100% acid stoichiometry run). The dissolution and reduction of mercury was very similar to that seen for Pd. The concentration of Hg and Pd are summarized in Figure 3-16.

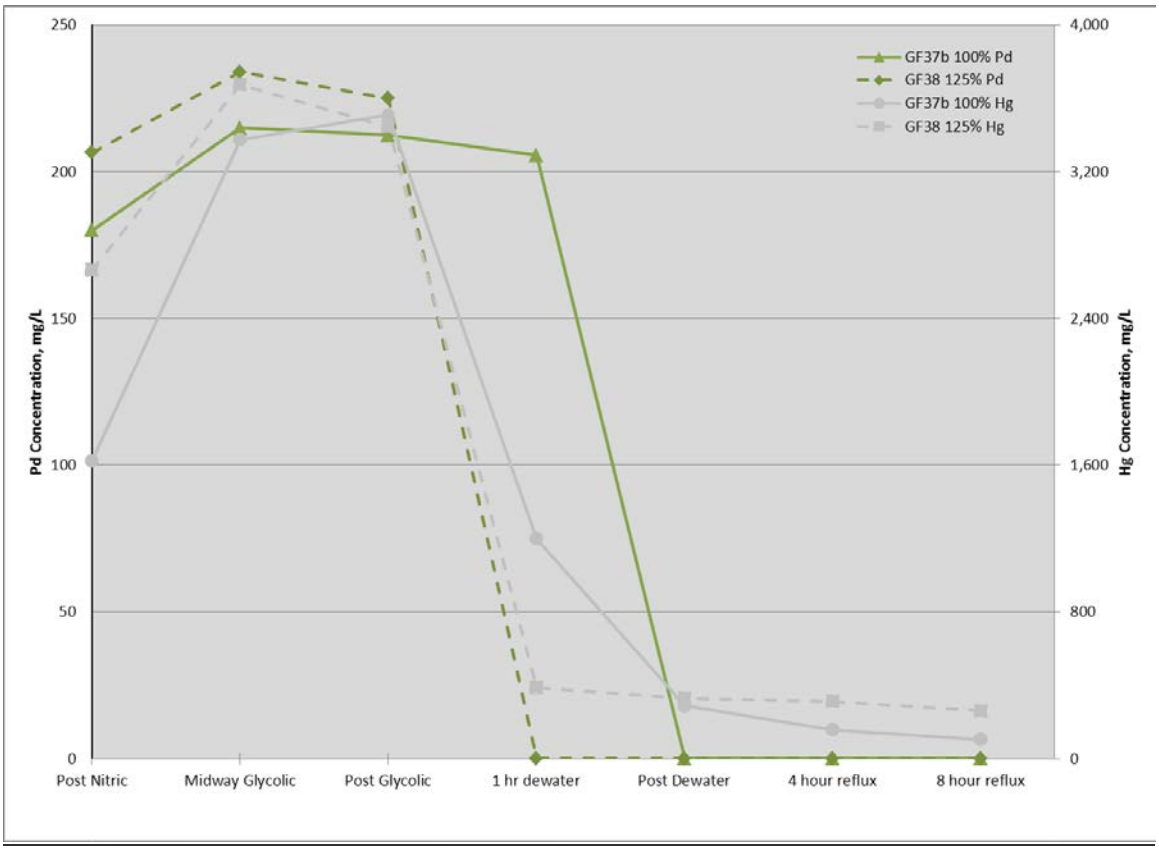

Figure 3-9. Mercury and Palladium Concentration for GF37b and GF38 SRAT Cycles

Mercury is being reduced by glycolic acid and approximately 30% of the mercury is removed from the SRAT by steam stripping and is collected in the MWWT. Approximately 40% of the mercury remains in the SME product. Another 4% was found in the condensate. There are two likely paths for condensate namely it can be removed by steam stripping (but not collect in the MWWT). This can happen in the SRAT cycle and SME cycle. In addition, the mercury can be dissolved by the strong acid in the condenser/MWWT condensate and overflow to the SMECT.

SRAT Elemental Data

General SRAT product slurry data for the twelve runs are tabulated below. Analyses were completed of both the slurry and supernate from all SRAT and SME products. The slurry results are summarized in Table 3-9. Conversion of the elemental data to the expected oxide form allows summing the oxides as a measure of both complete sample dissolution and accurate analysis of the major elements in the sludge product. The sum of oxides range from 98.2-100.5 over this data set (95-105 is considered acceptable). The slurry samples were filtered and the supernate results of these analyses are summarized in Table 3-10. The solubility of the cations is summarized in Table 3-11.

Table 3-10. SRAT Product Slurry PSAL Elemental Data, wt % calcined solids basis

Run	GF34	GF34b	GF34c	GF35	GF36	GF36b	GF36c	GF37	GF37b	GF38	GF40	GF41
Al	9.01	8.77	8.69	15.2	9.1	9.2	9.1	23.7	23.5	23.9	14.7	11.7
B	<0.100	NM	NM	<0.100	<0.100	<0.100	<0.100	<0.100	<0.100	<0.100	<0.100	<0.100
Ba	0.080	0.077	0.081	0.108	0.095	0.094	0.092	0.063	0.064	0.063	0.090	0.051
Ca	3.58	3.74	3.77	0.80	2.12	1.95	1.94	1.68	1.66	1.69	0.601	0.431
Cd	<0.010	NM	NM	<0.010	<0.010	<0.010	<0.010	<0.010	<0.010	<0.010	NM	NM
Cr	0.017	0.016	0.016	0.067	0.273	0.269	0.269	0.223	0.224	0.220	0.025	0.023
Cu	0.070	0.051	0.054	0.052	0.054	0.043	0.040	0.051	0.040	0.041	0.030	0.026
Fe	32.3	31.1	31.3	20.5	32.0	32.9	32.9	12.6	12.3	12.3	14.2	12.7
Hg@	1.27	0.82	0.89	0.02	0.65	0.81	0.87	0.83	0.59	0.92	0.52	0.52
K	0.080	0.087	0.118	0.075	0.061	0.077	0.083	0.071	0.079	0.086	0.412	0.442
Li	<0.100	NM	NM	<0.100	<0.100	NM	NM	<0.100	<0.100	<0.100	<0.100	<0.100
Mg	0.410	0.389	0.401	0.382	2.57	2.77	2.76	2.36	2.40	2.43	0.398	0.258
Mn	4.01	3.80	3.77	5.02	0.706	0.640	0.631	0.666	0.600	0.596	4.51	4.15
Na	14.2	13.8	13.9	15.5	13.5	13.4	13.2	15.3	14.1	14.4	23.0	26.1
Ni	0.212	0.182	0.189	3.42	2.69	2.73	2.73	2.37	2.35	2.37	1.95	1.55
P	<0.100	<0.100	<0.100	<0.100	<0.100	<0.100	<0.100	<0.100	<0.100	<0.100	<0.100	<0.100
Pb	0.080	0.069	0.071	0.023	0.056	0.049	0.041	0.058	0.050	0.039	<0.010	<0.010
Pd	<0.100	0.03	0.03	<0.100	<0.100	<0.010	<0.010	<0.100	<0.010	<0.010	<0.100	<0.100
Rh	0.031	<0.100	<0.100	0.032	0.033	<0.100	<0.100	0.047	<0.100	<0.100	<0.100	<0.100
Ru	0.032	<0.100	<0.100	0.031	0.032	<0.100	<0.100	0.030	<0.100	<0.100	<0.100	<0.100
S	0.276	0.282	0.281	0.347	0.276	0.264	0.269	0.294	0.283	0.260	0.292	0.341
Si	1.48	1.57	1.50	1.70	1.95	1.82	1.76	1.30	1.42	1.39	1.41	0.86
Sn	<0.010	NM	NM	0.029	0.107	0.102	0.102	0.089	0.094	0.093	NM	NM
Ti	0.010	<0.010	<0.010	0.025	0.010	<0.010	<0.010	0.010	<0.010	<0.010	0.022	0.012
Zn	0.062	0.063	0.065	0.064	0.072	0.071	0.070	0.061	0.062	0.062	0.046	0.039
Zr	0.055	0.051	0.054	0.236	0.117	0.110	0.110	0.045	0.040	0.044	0.201	0.178

@ Hg reported on a total solids basis

Table 3-11. SRAT Product Supernate PSAL Elemental Data, mg/L supernate basis

Run	GF34	GF34b	GF34c	GF35	GF36	GF36b	GF36c	GF37	GF37b	GF38	GF40	GF41
Al	292	1,060	1,230	217	411	2,280	2,250	554	2,210	4,040	1,720	1,970
B	1.22	NM	NM	1.28	1.23	<10.0	<10.0	1.49	<10.0	<10.0	<10.0	<10.0
Ba	2.18	4.33	4.44	0.99	1.65	3.28	3.32	1.26	2.69	3.37	9.37	11.0
Ca	2,390	4,150	4,200	109	2,390	3,350	3,490	2,150	3,040	2,870	368	403
Cd	<0.010	NM	NM	<0.010	<0.010	<0.100	<0.100	<0.010	<0.100	<0.100	NM	NM
Cr	2.58	4.34	4.85	3.52	32.0	54.8	53.7	86.0	103	198	27.4	29.8
Cu	11.6	20.8	23.0	1.33	11.9	25.9	24.6	15.1	24.7	38.5	19.4	21.9
Fe	1,670	4,470	5,220	141	1,040	2,810	3,290	328	1,490	3,560	5,510	4,950
K	392	303	422	321	272	16.4	5.23	290	265	247	918	985
La	27.8	NM	NM	2.84	18.6	239	269	39.2	NM	NM	<10.0	<10.0
Li	<10.0	NM	NM	<10.0	<10.0	<1.00	<1.00	<10.0	<1.00	<1.00	<10.0	<10.0
Mg	309	256	268	203	4,830	4,460	4,040	4,410	4,090	4,180	280	316
Mn	8,850	7,060	7,370	2,670	1,330	1,280	1,150	1,300	1,280	922	5,130	4,190
Na	30,100	24,900	15,400	33,700	26,500	28,200	25,900	30,400	29,800	28,500	44,300	47,800
Nd	7.13	NM	NM	0.61	4.58	10.77	9.84	10.71	NM	NM	NM	NM
Ni	121	117	123	100	2,940	3,160	2,850	3,160	3,180	3,960	732	659
P	0.86	<1.00	<1.00	1.04	1.13	1.54	1.86	1.56	<10.0	<10.0	14	20.6
Pb	4.10	4.73	5.14	0.17	0.61	2.29	2.01	2.31	4.15	18.9	6.73	9.91
Pd	0.16	0.123	0.122	0.21	0.16	0.18	0.13	0.18	<0.100	<0.100	<1.00	<1.00
Rh	2.97	15.9	10.4	9.21	10.7	18.4	15.0	12.0	36.0	78.3	30.5	31.4
Ru	106	174	125	25.6	181	229	206	289	330	453	54.1	65.9
S	645	439	446	880	572	453	482	672	599	513	583	622.7
Si	23.5	52.3	55.8	38.3	17.4	132	68.8	67.4	121	103	44.4	77.8
Sr	4.17	NM	NM	2.32	3.06	NM	NM	2.99	41.6	77.3	NM	NM
Ti	<0.010	<0.100	<0.100	<0.010	<0.010	<0.100	<0.100	<0.010	<0.100	<0.100	0.700	0.867
Zn	25.7	30.3	33.7	0.400	28.6	34.1	34.0	39.6	42.8	64.6	22.0	27.1
Zr	6.29	20.9	23.8	22.6	14.5	60.9	62.0	17.7	38.3	50.7	195	208

Table 3-12. Major Components: SRAT Product % of Element Dissolved

Run	Al	Fe	Na	Mg	Mn
GF34 HiFeHiMn	1.3	2.1	87.5	31.0	90.8
GF34b HiFeHiMn	0.0011	7.3	90.8	33.3	93.8
GF34c HiFeHiMn	0.0010	8.5	92.7	34.1	99.9
GF35SB7A	0.6	0.3	92.9	22.7	22.7
GF36 HiFeLoMn	2.0	1.5	88.2	84.0	84.6
GF36b HiFeLoMn	12.9	4.4	88.2	84.0	84.6
GF36c HiFeLoMn	12.7	5.1	108.6	83.2	103.4
GF37 LoFeLoMn	1.1	1.2	94.9	89.0	93.1
GF37b LoFeLoMn	4.8	6.3	108.8	88.1	110.2
GF38 LoFeLoMn	9.4	16.2	109.6	95.8	86.0
GF40	6.0	20.1	99.7	48.7	58.8
GF41	9.3	21.7	102	68.2	56.1

SRAT Anion Data

Ion Chromatography using weighted dilutions of samples (not the AD acid strike oxalate method) was performed on both the slurry and supernate from all SRAT and SME products. The slurry results are summarized in Table 3-12. The slurry samples were filtered and the supernate results of these analyses are summarized in Table 3-13. Anion balance data for nitrite, nitrate, formate and glycolate are presented in the table below for all runs (Table 3-14).

The SRAT and SME product oxalate results are of particular interest. The starting sludge contained about 800 mg/kg oxalate, which could be partially destroyed catalytically during the SRAT cycle. In the glycolic/formic flowsheet runs, however, oxalate was being created. The glycolic acid is likely oxidized to glyoxylic acid ($HCOCO_2H$) by nitrite, which is further oxidized to oxalic acid by the reduction of mercury. However, more experiments are needed to pinpoint the reaction pathways.

Table 3-13. SRAT Product Slurry PSAL Anion Data, mg/kg Slurry Basis

Run	Formate	Chloride	Nitrite	Nitrate	Sulfate	Oxalate	Glycolate
GF34	<100	650	<100	57,150	1,250	1,990	44,850
GF34b	<100	649	<100	54,450	1,910	4,970	46,450
GF34c	<100	717	<100	53,900	2,720	5,860	50,000
GF35	<100	572	<100	43,450	1,910	4,370	39,850
GF36	<100	622	<100	57,500	1,210	3,955	37,250
GF36b	<100	591	<100	56,650	1,280	3,190	51,250
GF36c	<100	602	<100	56,350	1,240	3,210	53,100
GF37	<100	821	<100	56,550	1,500	2,755	42,200
GF37b	<100	590	<100	52,500	1,445	2,420	55,450
GF38	<100	583	<100	56,900	1,420	2,655	77,850
GF40	<100	<500	<100	48,200	1,780	17,000	49,200
GF41	<100	<500	<100	41,700	1,220	13,300	48,600

Table 3-14. SRAT Product Filtrate PSAL Anion Data, mg/L Supernate Basis

Run	Formate	Chloride	Nitrite	Nitrate	Sulfate	Oxalate	Glycolate
GF34	<100	894	<100	80,500	2,250	1,570	56,300
GF34b	<100	806	<100	71,000	2,280	6,310	58,400
GF34c	<100	931	<100	70,900	3,520	7,730	66,500
GF35	<100	823	<100	63,700	2,790	3,800	48,600
GF36	<100	858	<100	86,300	2,170	3,250	46,700
GF36b	<100	736	<100	74,000	1,530	4,060	64,500
GF36c	<100	783	<100	74,300	1,610	4,240	70,700
GF37	<100	913	<100	82,100	2,740	3,860	61,300
GF37b	<100	772	<100	70,900	1,850	3,030	72,500
GF38	<100	746	<100	77,300	1,790	3,605	98,100
GF40	<500	<500	<500	60,400	1,910	11,100	50,300
GF41	<500	<500	<500	76,100	2,340	14,700	57,500

As a result of uncertainty of the anion analyses, four samples were submitted to AD for both TOC and anion analysis. The data below (Table 3-16) shows the results from both PSAL and AD for comparison. The agreement is fairly good, with the exception of the glycolate and oxalate. In addition, the carbon species (formate, oxalate, glycolate) were converted to carbon concentrations and summed to estimate the Total Organic Carbon (TOC) result for each sample. These results were compared to the AD measured TOC result. It is obvious that the TOC predicted from the PSAL results agreed well with the TOC measurement.

Table 3-15. % Anion Dissolved in SRAT Products

Run	Chloride	Glycolate	Nitrate	Oxalate	Sulfate	Sulfate (S)*
GF34	101.7	92.9	104.1	58.2	133.1	96.1
GF34b	99.6	59.3	98.7	41.6	114.8	78.5
GF34c	99.9	60.0	106.2	51.4	88.4	80.6
GF35	94.9	91.7	110.4	65.4	110.1	108.0
GF36	108.2	93.8	112.4	61.5	134.2	92.8
GF36b	98.5	97.9	101.6	99.0	92.9	88.9
GF36c	103.2	103.8	102.7	102.9	101.1	92.2
GF37	96.8	111.4	111.3	107.3	139.9	109.1
GF37b	101.3	101.8	105.2	97.7	99.4	109.6
GF38	104.8	98.3	105.9	105.8	98.5	109.6
GF40	85.2	60.1	94.1	61.1	103.6	103.4
GF41	101.9	65.5	94.4	93.8	157.2	101.7

* Sulfate (S) is a calculation of SO_4 from measured ICP-AES Sulfur analysis

Table 3-16. SRAT Product AD and PSAL Anion with Comparison to AD TOC, mg/kg

Analyte	GF36b	GF36c	GF37b	GF38
PSAL glycolate	50,200	55,100	55,500	77,900
AD Glycolate	33,900	34,400	35,900	54,500
PSAL Oxalate	3,160	3,300	1,340	2,390
AD Formate	<500	<500	<500	<500
PSAL Formate	<100	<100	<100	<100
PSAL Calculated TOC	20,900	24,100	24,100	32,400
AD Calculated TOC	11,500	11,500	11,900	18,100
AD Measured TOC	19,700	28,600	24,500	26,200

SME Elemental Data

General SME product sample data for the four runs (GF34, GF35, GF36 and GF37 had SME cycles) are tabulated below. The waste loading for these runs was targeted at 36% using frit 418. Elemental analyses were completed of both the slurry and supernate from all SME products. The slurry results are summarized in Table 3-22. Conversion of the elemental data to the expected oxide form allows summing the oxides as a measure of both complete sample dissolution and accurate analysis of the major elements in the sludge product. The sum of oxides range for 98.6-100.5 over this data set (95-105 is considered acceptable). The slurry samples were filtered and the supernate results of these analyses are summarized in Table 3-23.

Table 3-17. SME Product Slurry Elemental Data, wt % calcined solids basis

Run	GF34	GF35	GF36	GF37	GF40	GF41
Al	3.35	5.47	3.4	9.00	5.06	5.03
B	1.32	1.40	1.30	1.30	1.50	1.59
Ba	0.031	0.041	0.036	0.026	0.027	0.023
Ca	1.28	0.25	0.680	0.651	0.304	0.300
Cd	<0.010	<0.010	<0.010	<0.010	NM	NM
Cr	0.016	0.037	0.119	0.103	0.017	0.016
Cu	0.035	0.037	0.035	0.029	0.013	0.015
Fe	11.8	7.4	11.9	4.85	4.08	3.45
K	0.063	0.048	0.041	0.049	0.174	0.173
Li	2.20	2.31	2.27	2.18	NM	NM
Mg	0.152	0.145	0.924	0.858	0.115	0.102
Mn	1.44	1.79	0.231	0.220	1.35	1.13
Na	8.60	9.23	8.60	9.06	11.2	10.8
Ni	0.073	1.21	1.00	0.92	0.58	0.49
P	<0.100	<0.100	<0.100	<0.100	<0.100	<0.100
Pb	0.038	0.014	0.036	0.035	<0.100	<0.100
Pd	<0.100	<0.100	<0.100	<0.100	<0.100	<0.100
Rh	0.017	0.018	0.027	0.025	<0.100	<0.100
Ru	0.015	0.024	0.034	0.023	<0.100	<0.100
S	0.099	0.116	0.102	0.114	0.075	0.082
Si	23.35	24.3	23.45	22.9	25.0	26.2
Sn	<0.010	0.013	0.044	0.038	NM	NM
Ti	0.007	0.013	0.012	0.008	0.064	0.066
Zn	0.026	0.027	0.028	0.026	0.017	0.016
Zr	0.026	0.103	0.051	0.024	0.182	0.173

Table 3-18. SME Product Supernate Elemental Data, mg/L supernate basis

Run	GF34	GF35	GF36	GF37	GF40	GF41
Al	178	343	320	922	2,240	2,680
B	54. 0	55.0	48.0	47.2	<10.0	<10.0
Ba	2.22	1.06	1.68	1.35	14.3	16.5
Ca	2,090	169	2,110	1,960	399	419
Cd	<0.010	<0.010	<0.010	<0.010	NM	NM
Cr	1.93	7.03	34.6	69.4	35.3	37.7
Cu	5.82	3.16	12.8	16.7	27.0	28.8
Fe	1,280	326	1,200	973	10,100	12,250
K	396	311	252	212	991	1,095
La	18.2	10.2	17.6	36.6	NM	NM
Li	2670	216	234	183	352	376
Mg	315	223	4,660	3,460	5,230	4,680
Mn	8,610	3,620	1,280	998	46,300	52,800
Na	29,500	37,000	24,750	25,500	46,300	52,800
Ni	114	226	2,800	2,490	1,070	868
P	0.77	2.49	1.02	1.87	10.2	10.8
Pb	4.01	0.30	0.81	2.01	15.7	19.1
Pd	0.18	0.24	0.14	0.13	<1.00	<1.00
Rh	2.83	12.2	12.6	7.95	36.7	37.9
Ru	86.8	35.3	166	205	85	97
S	679	874	575	516	715	755
Si	30.6	102	27.6	71.5	62.3	86.7
Sr	4.22	2.67	3.05	2.77	NM	NM
Ti	<0.010	<0.010	<0.010	<0.010	0.938	1.194
Zn	20.6	2.40	28.4	17.0	41.9	44.2
Zr	5.25	38.0	32.1	22.2	261	258

SME Anion Data

Ion Chromatography was completed for both the slurry and supernate from all SME products. The slurry results are summarized in Table 3-24. The slurry samples were filtered and the supernate results of these analyses are summarized in Table 3-25. Anion balance data for nitrite, nitrate, formate and glycolate are presented in the table below for all runs (Table 3-26).

The anion data is inconsistent. For example, in Run GF37, the data indicates there was high nitrite to nitrate conversion in the SRAT and high nitrate loss in the SME. Also, it indicates that glycolate was destroyed in the SRAT and generated in the SME. It is more likely that there was a lower nitrite to nitrate conversion and lower glycolate loss in the SRAT with minimal nitrate and glycolate loss in the SME. The inconsistent results is likely due to fouling of the IC columns by metals and oxalate that are soluble at pH 4 but insoluble at pH 10 (approximately sample of eluent). It is recommended that removal of metals with an appropriate guard column be considered. An anion round robin has been initiated to resolve the issues with the analytical technique.

Table 3-19. SME Product Slurry Anion Data, mg/kg Slurry Basis

Run	GF34	GF35	GF36	GF37	GF40	GF41
Chloride	525	445	494	821	500	500
Nitrite	<100	<100	<100	<100	<100	<100
Nitrate	43,650	34,750	43,650	56,550	48,200	41,700
Sulfate	1,060	1,470	1,000	1,500	1,780	1,220
Oxalate	1,670	3,290	4,150	2,755	17,000	13,300
Glycolate	37,250	30,750	28,200	42,200	49,150	48,600
Formate	1,405	2,330	1,720	<100	<100	<100
Phosphate	<100	<100	<100	<100	<100	<100

Table 3-20. SME Product Filtrate Anion Data, mg/L Supernate Basis

Run	GF34	GF35	GF36	GF37	GF40	GF41
Formate	<100	<100	<100	<100	<500	<500
Chloride	892	770	884	726	<500	<500
Nitrite	<100	<100	<100	<100	<500	<500
Nitrate	79,100	58,200	84,750	60,100	94,000	84,000
Sulfate	2,345	2,825	2,710	2,570	2,330	2,540
Oxalate	1,620	4,845	3,960	3,395	10,400	13,500
Glycolate	59,400	42,150	45,550	45,600	60,400	58,500
Formate	1,715	3,785	2,251	1,940	<500	<500
Phosphate	<100	<100	<100	<100	<500	<500

SME Condensate

The SME condensate was not analyzed for GF34-38. However, GF40 and GF41 SME condensate samples were collected. Each sample was analyzed for elementals via ICP-AES, and anions via IC. The condensate was very low in anions and cations. The largest component is the silicon, likely an antifoam degradation product, not frit, as the same concentration was seen in the SRAT condensate. Note also that the pH of the SME condensate is considerably higher than the SRAT condensate. The SME dewater results are summarized in Table 3-27.

Table 3-21. SME Condensate, mg/L

Analyte	GF40	GF41
Hg	24.6	15.4
K	14.6	14.5
Na	15.3	8.62
Si	1,455	553
Ti	<1.00	<1.00
NO_3^-	329	125
Density	0.9976	0.9970
pH	3.28	3.39

Note: The following were less than detection limits: Al, Ca, Cr, Cu, Fe, Mg, Mn, Ni, P, S, Ti, Zn, Zr, NO_2^-, SO_4^{2-}, $C_2O_4^{2-}$, $C_2H_3O_3^-$, HCO_2^-

Other SME Data

Other SME product data are summarized in the Table 3-28. Of particular note is that the GF37 SME was not completed prior to kettle breakage. As a result, the total solid result of the recovered product is significantly lower than had been targeted. Also, no analyses were completed on the SME condensate from Runs GF34-GF37.

Table 3-22. Other SME Product Data

Run	GF34	GF35	GF36	GF37	GF40	GF41
Total Solids, wt%	48.8	46.3	45.8	39.3	49.8	54.0
Insoluble Solids, wt%	37.9	37.6	35.3	29.7	36.9	41.0
Calcined Solids, wt%	38.5	37.3	35.8	29. 7	38.0	42.9
Soluble Solids, wt%	10.9	8.71	10.5	9.53	12.9	13.0
pH	4.66	6.18	4.39	4.31	4.76	4.81
Slurry Density, g/mL	1.42	1.34	1.38	1.29	1.137	1.150
Supernate Density, g/mL	1.11	1.10	1.10	1.09	1.243	1.234
Ammonium, mg/L	14	<5	<5	7	<10	<10

Note: GF40 and GF41 SME products were too thin and the frit settled quickly. It was difficult to maintain a uniform mixture. Higher total solid targets are recommended in future processing of underwashed sludges as significantly less insoluble solids are present in the SME product, as the sodium is included in the waste loading calculation.

SRAT Supernate Chemistry

The composition of the SRAT product slurry and supernate anions is summarized in Table 3-12, Table 3-13. SRAT Product Filtrate PSAL Anion Data, mg/L Supernate Basis and Table 3-14. Figure 3-18 and Figure 3-19 show the amount of each element found in the SRAT product supernate expressed as a percentage of the total element present. These data are calculated by dividing the supernate concentration (converted to mg/kg on a slurry basis) by the total slurry fraction of each element (converted to mg/kg). Numbers greater than 100% are not physically possible and are a result of error in one of the analytical measurements used in the calculation.

The % solubility of each anion is approximately 100% (80-120% based on method uncertainty), except for oxalate, which had a solubility of approximately 60% in the GF34 and GF35 runs. The solubility of Al and Fe was low in all runs. The solubility of Na, Mg, and Mn are all high in the glycolic flowsheet runs. For most of the metals, which are present primarily as hydroxides and oxides in the sludge, the concentration in the supernate increases throughout the SRAT cycle, but appear to be constant by the end of the SRAT cycle. Samples were pulled at the completion of nitric acid addition, midway through glycolic acid addition, after completing glycolic acid addition, one-hour into dewater, post dewater, 4 hours into reflux and 8 hours into reflux. These samples were centrifuged soon after being pulled to make sure no further reactions occurred due to insoluble solids. One interesting observation is that the centrifuged GF37b samples (100% acid stoichiometry) had almost no supernate after centrifuging at the completion of dewater (0.3 g of supernate typical in these samples). Prior to dewater and throughout run GF38 approximately 6-7 g of supernate was easily removed after centrifuging.

Based on this data, the order of dissolution for the "major components" is: Hg>Ca>Mn>Ni>Mg>Al>Fe. The data is summarized for major metals (>1,000 g/L) in Figure 3-18 and minor metals in Figure 3-19. The graphs show the approach to maximum solubility, defined as 100% for each element on these graphs. This does not indicate that 100% of these individual elements went into solution during processing.

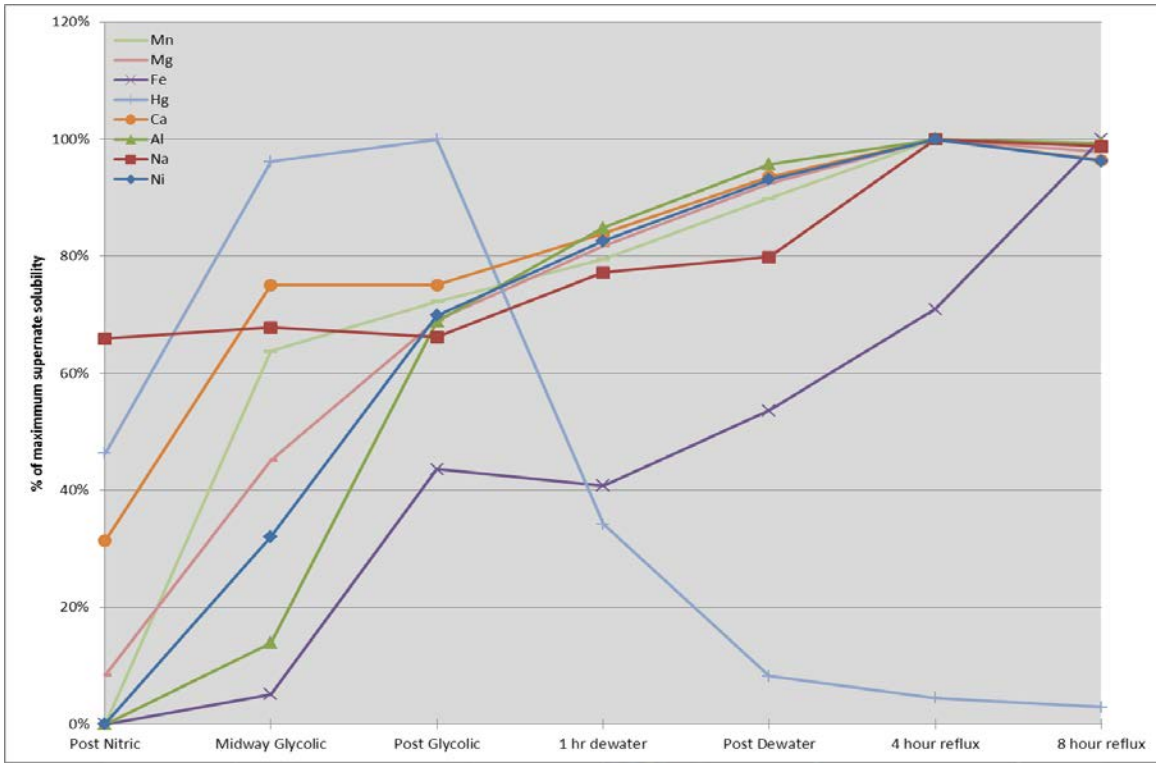

Figure 3-10. Order of Dissolution of "Major Metals" During SRAT Processing

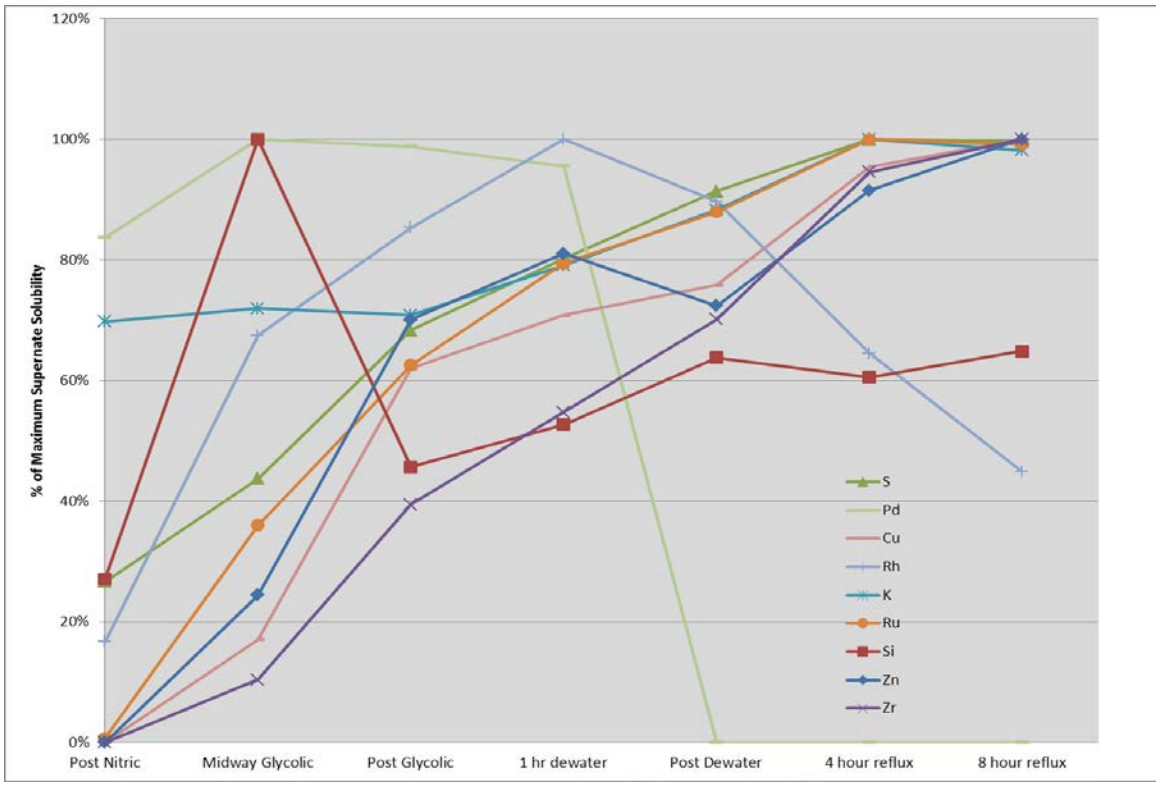

Figure 3-11. Order of Dissolution of "Minor Metals" During SRAT Processing

Several metals are of particular interest during SRAT processing. Note that mercury is discussed in Section 3.2.2. The reduction of Mn is important especially in the melter and cold cap in order to minimizing foaming in the melter. As can be seen in Figure 3-18, the Mn is dissolved (and likely reduced) early in the SRAT cycle and is >90% of the maximum solubility by the end of dewater. There are several metals that are essentially totally soluble such as Na, K, and Ca. The concentration of each metal changes as the metal is first diluted during acid addition, then concentrated during the dewater phase. In addition, the concentration of soluble metals should remain constant throughout the post dewater stage of the SRAT cycle. In GF37b, the concentration of both Na and Ca increased during this time, likely due to the extended centrifuge time necessary to squeeze out the 0.3 g of supernate from a 15 mL centrifuge tube. Note that for the lower acid run, GF37b, the calcium was not completely soluble until midway through glycolic acid. This may indicate that it may take more than 100% acid stoichiometry to produce a SRAT product that is easily concentrated in the SME.

In order to understand the dissolution of metals and the timing of their dissolution, additional samples were pulled during runs GF37b and GF38 (LoFeLoMn sludge). The dissolution of Hg is discussed in the mercury section.

SME Supernate Chemistry

The main change in supernate chemistry during the SME cycle is that formic acid is added to the frit slurry to prevent caking. Formic acid is very reactive in DWPF SRAT and SME processing, ultimately leading to the noble metal catalyzed decomposition to hydrogen and

CO_2. No formic acid was added or detected during the SRAT cycle. The solubility of the anions during the SME cycle is summarized in Table 3-29.

Table 3-23. Major Components: SME Product % of Anion Soluble

Run	GF34	GF35	GF36	GF37	GF40	GF41
Formate	68.1	92.5	76.7	67.4	NA	NA
Glycolate	89.0	78.1	94.6	95.8	62.4	57.6
Nitrate	101	95.4	114	101	99.0	96.5
Oxalate	54.1	83.9	55.9	77.4	31.1	48.6
Sulfate	123	109	159	136	66.4	99.7
Sulfate (S)	98.9	115.0	91.9	98.4	128	103

* Sulfate (S) is a calculation of SO_4 from measured ICP-AES Sulfur analysis

Conclusions

Testing was completed to demonstrate the viability of the newly developed glycolic/nitric flowsheet for processing in the Defense Waste Processing Facility's (DWPF) Chemical Process Cell (CPC). The Savannah River National Laboratory (SRNL) initiated a sludge matrix study to evaluate the impact on CPC processing. Four sludge simulants were designed to cover a broad insoluble solid composition range to bracket future sludge batches. The first pair of sludge parameters was high iron/low aluminum versus low iron/high aluminum (referred to as HiFe or LoFe in this report). The second pair of sludge parameters was high calcium-manganese/low nickel, chromium, and magnesium versus low calcium-manganese/high nickel, chromium, and magnesium (referred to as HiMn or LoMn in this report). In addition, a simple supernate simulant was prepared to match the composition of the matrix simulants.

Ten experiments (GF34 to GF37 and GF34b, GF34c, GF36b, GF36c, GF37b and GF38) were completed to demonstrate the glycolic-nitric flowsheet viability using the sludge matrix simulants. In addition, two experiments were performed with less washed simulants (GF40, 2M and GF41, 2.5 M Na endpoints) to demonstrate the viability of processing these sludges. Also, five supernate experiments (GF39a-GF39eGF39e) were performed to better understand the reaction sequence, particularly the reduction and stripping of mercury.

Composition and physical property measurements were made on the Sludge Receipt and Adjustment Tank (SRAT) and Slurry Mix Evaporator (SME) products. Composition measurements were made on the composited condensates from the Mercury Water Wash Tank (MWWT), and Formic Acid Vent Condenser (FAVC), on the ammonia scrubber solution, and on SRAT samples pulled throughout the SRAT cycle. Updated values for glycolate and formate loss, nitrite-to-nitrate conversion, and oxalate formation were found that can be used in the acid calculations for future process simulations with the glycolic-nitric flowsheet.

Preliminary results of the initial testing indicate:

- Hydrogen generation rate was below detection limits (<11.4E-3 lb/hr DWPF-scale or <0.005 vol%) throughout all SRAT cycles with matrix simulants. Hydrogen generation rate was above detection limits for the less washed simulants (3.2E-3

lb/hr DWPF-scale or 0.009 vol%) due to the higher acid stoichiometry and the lower offgas purge.

- Hydrogen generation rate was below 0.0258 lb/hr DWPF-scale throughout all SME cycles with matrix simulants. Hydrogen was produced in the matrix SME cycles because formic acid was added with the frit slurry. Hydrogen generation rate was above detection limits for the less washed simulant in GF40 (1.8E-3 lb/hr DWPF-scale or 0.007 vol%) but was below detection limit in GF41 due to the higher acid stoichiometry and the lower offgas purge. No formic acid was added in runs GF40 and GF41.
- Mercury was both reduced and stripped without formic acid. The mercury concentration of the SRAT product was below the 0.8 wt % limit in eight of the runs and below 0.92 wt % in the other four runs.
- Nitrite in the SRAT product was <100 mg/kg slurry for all runs.
- Foaminess was not an issue using the nominal antifoam addition strategy or with reduced antifoam in these tests.
- High wt % total solids were achieved while staying within rheological limits which makes the glycolic acid/nitric acid flowsheet an improvement for processing more viscous sludges. However, there may be a tradeoff between excessive dissolution of metals and thinner rheology.
- The pH remained steady throughout processing (i.e. no pH rebound) potentially leading to more consistent processing during the CPC. The SRAT and SME products pH varied from 3.5-5.0 for the 100% and 130% acid stoichiometry runs, significantly lower than is typical of the Baseline nitric acid/formic acid flowsheet.
- The testing apparatus has been significantly modified to improve processing with high viscosity slurries. Testing of the old style and new style rig identified no differences in CPC processing, including steam stripping of Hg.
- The SRAT lower air purge was demonstrated in Run GF34c and used in GF40 and GF41. The SRAT purge can be reduced from 190 scfm to 93.7 scfm without negatively impacting DWPF CPC processing.
- Runs GF40 and 41 demonstrated that processing of less washed sludges is viable with the Glycolic-Nitric flowsheet. However, this flowsheet has not been demonstrated with ARP, MCU or actual waste.
- Several processing improvements were demonstrated in these runs including adding acid during heat-up, adding both acids at higher volumetric flowrates than are currently used in DWPF, and concentrating the SRAT during acid addition. Each of these improvements has the potential to shorten CPC processing time.

Recommendations

The glycolic-nitric flowsheet is recommended as a viable flowsheet alternative to the Baseline DWPF flowsheet. In the testing that has been performed to date, this flowsheet meets or outperforms the current flowsheet in minimizing off-gas generation, removing mercury, and producing a rheologically thinner product. Previous testing with glycolic/formic acid mixtures demonstrated a wide processing window regarding both the glycolic-formic ratio

and acid stoichiometry. The addition of glycolic acid leads to SRAT products that are rheologically less viscous which means that more concentrated products can be produced, leading to potentially higher waste throughput per batch. In addition, the combination of lower pH processing and the complexing power of glycolic acid leads to the dissolution of more metals, which may minimize deposits in the CPC processing vessels and prevent the fouling of steam coils. Follow-up testing is recommended in the following areas:

- Improve glycolate and oxalate analyses. The majority of the glycolate results reported were correct. However, there are issues with anion and cation deposition on the column of the Ion Chromatograph (IC), causing higher than expected glycolate and oxalate in blanks and some samples. Both Process Science and Analytical Laboratory (PSAL) and Analytical Development (AD) have reported results that have varied significantly from expectations. Modification to the sample preparation method is likely needed to improve analytical accuracy and minimize the cleaning and replacement of the IC column. An alternative to the IC measurement of glycolate should also be considered.
- Determine the appropriate REDOX model for the glycolic-nitric flowsheet. The REDOX model may need more terms due to the more extensive reduction of some metals, including Mn and Fe. In addition, accurate measurement of glycolate (and possibly oxalate) and nitrate is needed to accurately predict REDOX. REDOX testing of the matrix sludges should be repeated using acceptable frits that meet Product Composition Control System (PCCS).
- Testing should be completed with alternate forms of ruthenium to determine whether the elimination of the chloride added as ruthenium chloride would improve the reduction and stripping of the mercury. Comparison testing should be completed with the Baseline and glycolic-nitric flowsheets.
- Test the glycolic-nitric flowsheet at acid stoichiometries of less than 100%. Demonstration of this flowsheet at an acid stoichiometry of <100% is recommended and might be useful for mercury stripping.
- Demonstrate the glycolic-nitric flowsheet (previously demonstrated in SRAT cycle with 80:20 glycolic:formic acid blend) with actual waste in SRNL Shielded Cells SRAT and SME processing, to include periodic slurry sampling throughout the SRAT and SME processing along with a glass REDOX measurement.
- Add the nitric and glycolic acid flowrate at the same scaled molar flowrate as formic acid to minimize glycolic-nitric flowsheet batch time.
- The nitric acid can be added during heat-up to decrease the SRAT cycle time. The nitric acid primarily neutralizes soluble the base species in the slurry with little offgas generation.
- Improve understanding of process chemistry, the decomposition of glycolate and the production of oxalate which are important to REDOX.
- Improve understanding of mercury reduction, stripping and accumulation during processing. Determine whether alternative equipment or processing changes are needed to maximize the collection of mercury in the Mercury Water Wash Tank.

- If confirmed by actual waste testing and larger scale testing with simulants, the antifoam addition can be reduced for this flowsheet. The addition of 100 mg/kg prior to glycolic acid addition, 100 mg/kg prior to boiling and 100 mg/kg each 12 hours of processing was adequate during simulant testing.
- More rigorous data collection is needed to validate the OLI aqueous model's solubility predictions with sample results. The methodology is summarized in the discussion.